ISSN: 2639-7455

Research Article

Earth & Environmental Science Research & Reviews

Finite Element Method of the Influence Evaluation of the Percentage of Fine Particles of Marine Clay at the Different Depth Variations to the Total Volumetric Strain of the Soft Clay Ground

Thy Truc Doan

Dept. of Technology and Engineering, Kien Giang University, Vietnam

***Corresponding Author**
Thy Truc Doan, Department. of Technology and Engineering, Kien Giang University, VietNam.

Submitted: 2023, Mar 27 **Accepted**: 2023, Apr 28 **Published**: 2023, May 09

Citation: Thy, T., D. (2023). Finite Element Method of the Influence Evaluation of the Percentage of Fine Particles of Marine Clay at the Different Depth Variations to the Total Volumetric Strain of the Soft Clay Ground. *Envi Scie Res & Rev, 6*(3), 460-469.

Abstract

Finite element method of the influence evaluation of the percentage of fine particles of marine clay at the different depth variations to the total volumetric strain of the soft clay ground is determined by the Viet Nam standard TCVN 4196:2012; TCVN 4102:2012; TCVN 4197:2012; TCVN 4199:2012. Results show clearly the percentage of the fine clay particle and the total volumetric strain (ε) with depths. The minimum value of 12% and 0.00002617 at 19.3m depth; whereas the maximum value of 38% and 0.00002609 at 25.3m depth. Moreover, a consideration of the relationship between Internal friction angle, Cohesive force, Water content, Saturation, Porosity, Viscosity, and Plasticity index with depths. Results show remarkably the increasing of the depths as the variations of the percentage of fine particles of marine clay and cohesive force, viscosity, water content, and porosity; compared with the decrease of the plasticity and internal friction angle. It is easy to conclude that the total volumetric strain of the soft clay ground is a stable and safe state to use and design the building, construction, and reference of engineers, geologists, scientists, and so on in the future.

Keywords: Percentage of Fine Particles of Marine Clay, Total Volumetric Strain, Water Content, Saturation, Viscosity, Plasticity Index, Porosity, Groundwater Levels with Depths

1. Introduction

In recent decades, there are much research on the percentage of fine clay particles with other characteristics from other researchers in the world by the different methods which shew in experiment and simulation measurements. A volumetric strain modification of the soil-water retention curve was used to determine the unsaturated soils by the experiment and simulation methods. Results presented the volumetric strain defined on the pore size distribution and the retention curves during wetting-drying cycles [1]. On the other hand, an element finite method is used to simulate the strain of soil by characteristics Spectroctro of polymer which was defined on terahertz. Results shew shock wave created laser on polymer as consideration of polymer of particle. However, there is any determination of porosity, water content, or saturation with depths. Moreover, a coupled computational fluid dynamics-discrete element method (CFD-DEM) was used to analyze the flow velocity and fine particle size to the porosity of the material. Results presented the decreaseof the fine particles as the flow speed through the flow velocity and fine size is small. In addition, it is necessary to develop flow speed and permeability increased with the bigger size of the particles [2]. However, an investigation of the stress and the fine particle by the glass fiber. The replaced materials shew 0%, 5%, 10%, 15%, 20% và 25% glass and irion filing which is according to water-cement with 0.55. Results presented the increasing of iron filings which made decreasing of stress and working capability at the optimal state [3]. A numerical model was used to calculate the propagation of micro-particle to credit deformation of structures of composite. Results shew breaks with the loading curves [4]. Experiment method was used to determine the volumetric and water retention behaviors of a compacted clay during soaking and desiccation considering the influences of freeze-thaw (FT) cycles and saline intrusion. Results presented the increasing of saline concentration as the shrinkage increased gradually [5]. An experiment method to control the volumetric strains by changing the suction or stress of an expansive bentonite/silt mixture treated with lime using an odometer machine. Results presented that at different suction forces (2, 4, and 8 MPa), suction increased and fine particles of bentonite became swelled larger than with no loading [6]. Full-field measurements of strain loclocalization sandstone by neutron tomography and 3D-volumetric digital image correla-

tion were used to determine clearly the deformation of sandstone. Results of the pre or post-deformation neutron tomography of a Bentheim sandstone sample at ex-situ at the loading of 40 MPa. This shows that the internal structure can be obtained for 3D-DIC and the 3D strain field [7]. An investigation of the Extra-fine dry powder inhalers to reach the smaller airway. Results presented poorly water-soluble meloxicam which decreased the particle size into the nano range by wet milling and producing extra-fine inhalable particles via nano spray-drying. the diameter of the drug was reduced to 138 nm. The dry particle size was obtained from 1.1 and 1.5 µm; whereas the dispersed diameter was shown from 500 and 800 nm [8]. A weight parameter was added to calculate the extended strain energy of bulk metallic glasses materials. Results presented the crack appeared much more as consideration of microscopic separation in materials [9]. An experimental method of strain-dependent SWRC (soil water retention curve) was used for the calculation of a hypothesis related to the changing in the pore size distribution (POSD) by the volumetric strain of soil skeleton. The result presented at initial degrees of saturation higher than 0.8, the influence of volumetric strain may be marginal whilst compared wtheh he initial degrees of saturation lower than 0.8 [10]. The research on concretegranite by the experiment method was used to determine strain and cracks. The results show the accuracy of the model with the experimental curves of the concretegranite obtained over 95% [11]. it had little effect on other changes caused by fine particles. Based on the results described above, we propose that fine particles in surgical smoke and atmospheric fine particles exhibit similar levels of toxicity toward embryonic development. Fine particles in surgical smoke potentially affect the beating of cardiomyocytes by damaging mitochondria and increasing oxidative stress.

2. Materials and Standards

Soil samples were collected carefully in the Field and moisture to ensure the natural state. The ground is soft clay with original marine clay, which is divided into 4 layers with plasticity to a hard state. On the other hand, there are two boreholes HK1 and HK2, which show depths from 2.5m to 25.3m of HK1 borehole; whereas borehole HK2 is from 1.5m to 21.8m. The total ground depth is 25.3m. The groundwater is located in +0.3m. Moreover, soil properties were shown in Table 1.

Layers	Depths (m)	Water content W (%)	Unit-specific weight on the groundwater level γw (kN/m³)	Unit-specific weight under the groundwater level γđn (kN/m³)	Plasticity index Ip (%)	Internal friction angle φ (⁰)	Cohesion force C (kNm²)	Descriptions
Standards		TCVN 4196:2012	TCVN 4102:2012		TCVN 4197:2012	TCVN 4199:2012		Viet Nam standard (TCVN)
1	4.3	23.08	19.23	9.82	14.62	16021’	30.4	Mid-clay, grey–white color; hard-plasticity.
2	9.8	22.16	19.4	1.0	15.18	17001’	35.8	Mid-clay, grey–white mixed brown red color; mid–hard state.
3	19.3	20.82	19.54	1.015	13.52	18048’	30.2	Mid-clay, brown-red color; mid–hard state.
4	25.3	24.42	1.909	0.971	20.04	16020’	49.8	Mid-clay, brown-yellow color; mid–hard state.

Table 1: Soil properties with the medium values (TCVN 4196:2012; 4102:2012; 4197:2012; 4199:2012)

3. Methodology

Experiment measurement in the laboratory at Kien Giang CIC Group has been done carefully to obtain the best results. The experiment of the water content W (%), unit-specific weight, and plasticity index was determined by the Viet Nam standard (TCVN 4196:2012; TCVN 4102:2012; and TCVN 4197:2012).

3.1 The Percentage of the Fine Clay Particle and Internal Friction Angle, Cohesive Force with Depths

The experiment to determine the cohesive force and internal friction angle was done by the Direct Shear Test with TCVN 4199:2012. The specification characteristics of the direct Shear machine was shown in Table 2. The 19 samples were measured with sizes 30cm² diameter. All of the samples were sieved with a sieve size < 0.005mm and moist within 24 hours before determination and measurements. A spring sample was used to contain the soil sample; then it was put clearly in the shear machine. The machine was operated by the Electric motor 220V/50Hz with a speed of 0.8mm/minute. After finishing the machine opening process, the soil sample was tightened on the machine and the shear pressure began loading at 100 (kN/m²); 200 (kN/m²); 300 (kN/m²). The results recording process was done after finishing of shear process and the sample is deformed. The Excel software is used to collect data, draw the figures and calculate the results (see Figure 1). The cohesive force with depths was done in formulas 1,2, and 3.

$$\tau_{max} = R_{coefficient} * K \quad (1)$$

$$\varphi = arctg \frac{\tau_{max}}{\sigma_{1,2,3}} \quad (2)$$

$$C = \tau_{max} - \sigma_{1,2,3\, x\, tg\varphi} \quad (3)$$

Whereas τ_{max} is the maximum value of the direct shear test where the sample is deformed with the maximum loading.

$R_{coefficient}$ is an actual value that is determined on the machine.
K is the spring coefficient of the machine (kN/m²).
φ is the internal friction angle which is a relationship between the maximum shear stress (τ_{max}) and pressure levels ($\sigma_{1,2,3}$). The pressure level ($\sigma_{1,2,3}$) includes σ^1 = 100 (kN/m²); σ_2 = 200 (kN/m²); σ_3 = 300 (kN/m²). C is cohesive force (kN/m²).

Sample area (cm²)	Spring coefficient (kN/m²)	Shear pressure (kN/m²)	Pressure levels (kN/m²)	Loading	Force fram (kN)	Clock (mm)
30	1.724	100; 200; 300	100; 200; 300; 400	Electric motor 220V/50Hz with speed 0.8mm/minute	1.2	10x0.01

Table 2: The specification characteristics of the direct Shear machine EDJ-I (TCVN 4199:2012)

3.2 The Percentage of the Fine Clay Particle and Plasticity Index and Viscosity with Depths

The percentage of distribution of the fine particle component with depths was done by TCVN 4198:2012. A total of 19 samples were collected at different depths by the Standard Penetration machine. The samples were dried outdoors after 72 hours and sieved with a standard sieve size < 0.005mm. The Excel software is used to collect data, draw the figures and calculate the results.

3.2.1 The Liquid Limitation with Depths

a) Humidity, W (%)

The humidity, W (%) is calculated according to the formula below:

$$W = \frac{m_1 - m_2}{m_2 - m} x100\% \quad (4)$$

Whereas: w is the humidity of soil (%).
m1 is wet mass at the initial state (g)
m2 is a dry mass (g) after being dried in the oven at t0 = 1050C temperature within 24 hours
m is the mass of a container of soil (gram)

b) The Liquid Limitation (W_L) with Depths

Place the soil sample on the tempered glass and use two knives to mix soil particles together to ensure uniform soil. Observe uniform particles and color soil, and if the soil is too dry or wet not to be used, we add water or dry it. Use a little soil mass and put it into the can, press the knife spread out evenly top to end surface of the can until full soil and clean the remaining soil on the surface of the can to create an absolutely flat can surface. Place the can on the balance cone and fix the can to a stable state. Place the nose of the cone at the contact surface of the top surface of the soil sample. The cone is dropped at a freedom state of how to come through 10 millimeters in a duration of 10 seconds. Repeat steps from step if it is not enough 10 millimeters per 10 seconds.

3.2.2 The Plasticity (WP) Limitation with Depths

Place soil on the glass and use two knives to mix the soil evenly. Observe the soil to ensure even color if the soil is too dry or wet, we must add water to or dry it. Place soil on the glass and roll the soil rod until the soil becomes a rod this rod has 3-millimeter diameters and it is very suitable for the rod length from 3 millimeters to 10 millimeters. Repeat the steps from 1 to 3 until soil appears to break on the rod surface and the rods are broken into about 10 short segments. Use broken segments and put them into the cans and cover them with the lid ensuring the soil is at the initial state. Repeat steps until soil mass reaches 10 grams. Bring soil can to the oven to dry with temperature t^0 = 105ºC and time 24 hours. Weigh the soil can again after drying from the oven to determine the humidity.

3.2.3 The Plasticity Index (IP) with Depths

The plasticity index (Ip) of soil is calculated by the formula below :

$$I_P = W_L - W_P \quad (5)$$

Whereas: IP is the liquid index of soil (%)
W_L is the liquid limit of soil (%).
W_P is the plasticity limit of soil (%).

3.2.4 The Viscosity (B) with Depths

The viscosity index of soil is calculated by the formula below:

$$B = \frac{W - W_P}{W_L - W_P} \quad (6)$$

4. Results and Discussion

4.1 The Percentage of the Fine Clay Particle and Internal Friction Angle, Cohesive Force with Depths

At the 9.3m depth, the percentage of the fine clay particle obtained the minimum value of 12%, which is according to the maximum values of the internal friction angle of 18.480 and cohesive force of 30.2 kN/m²; whereas compared with the minimum value of the percentage of the fine clay particle 38% at 25.3m which is according to the minimum value of the internal friction angle 16.20 and the maximum value of the cohesive force is 51.1kN/m².

On the other hand, at the lowest depth which shows the nearest location of the ground, the percentage of the fine clay particle obtained a value of 14.5%, which is according to the values of the internal friction angle of 15.53º and cohesive force 29.3 kN/m2. Moreover, the percentage of the fine clay particle varied clearly and unevenly at the different depths such as 14.5%; 13.5%; 18.0%; 14%; 21%; 13%; 26.5%; 16%; 15.5%; 15.5%; 20%; 13.5%; 17%; 14%; 20%; 35%; 37% at 1.8m; 2.8m; 4.3m; 5.3m; 6.3m; 9.3m; 9.8m; 11.8m; 12.8m; 14.5m; 15.3m; 16.8m; 17.8m; 19.3m; 21.8m; and 22.8m; which is according to the internal friction angle 17º.14'; 14º.58'; 17º.1'; 16º.34'; 17º.41'; 16º.47'; 17º.1'; 18º.35'; 17º.14'; 18º.48'; 15º.53'; 16º.47' and the cohesive force 28.2 kN/m²; 35.6 kN/m2; 32.2 kN/m2; 38.2 kN/m2; 29.9 kN/m2; 37.4 kN/m2; 35.3 kN/m2; 28.2 kN/m2; 41.4 kN/m2; 32.2 kN/m2; 44.0 kN/m2; 33.9 kN/m2; 41.4 kN/m2; 46.6 kN/m2; 51.7 kN/m2. So it is easier to conclude that the percentage of the fine clay particle varied remarkably and unevenly. The maximum value was obtained at the maximum depth of 25.3m (see Figure 1). This resulted in the total volumetric strain (ε) is not big value, so the soft clay ground is stable with the building loading. 4.2.2. Porosity with Depths

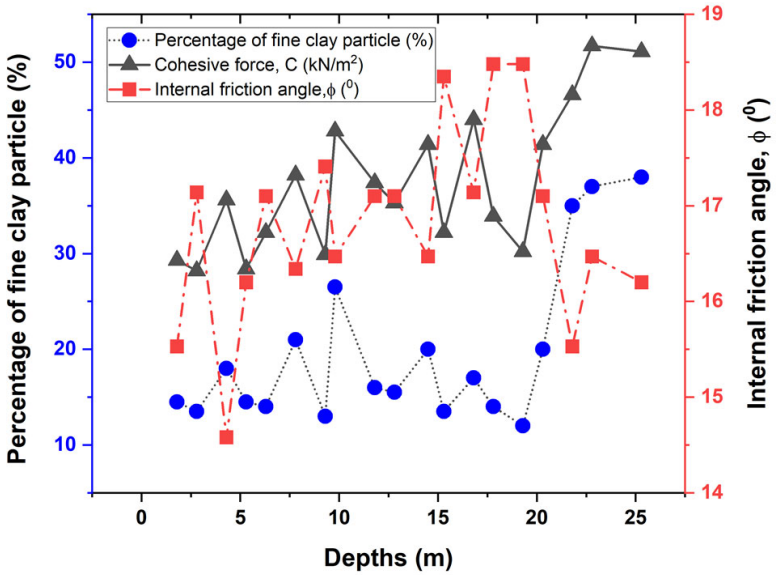

Figure 1: Results of the percentage of the fine clay particle and depths as consideration of the Internal friction angle and Cohesive force

However, Thy Truc Doan, 2023 the results of the evaluation of the internal friction angle of the clay with the river's original shew clearly in Table 3. The medium value of the internal friction angle is 23.08º 24.25' from 18.3m to 39.3m depths. And the mean value at the center of the ground was obtained at 9.58º 8.08'; which is according to the medium diameter of the particle is from < 0.005mm to 0.5mm.

Types of soil	Depths (m)	(ϕº)	Depths (m)	(ϕº)
Clay layer (The medium diameter is from < 0.005mm to 0.5mm)	0.0m ÷4.0m	2º60'	14.0m ÷15.0m	16º34'
	4.0m ÷ 4.5m	2º28'	18.0m ÷20.0m	18º22'
	4.5m ÷ 5.0m	1º58'	20.0m ÷21.0m	16º34'
	7.0m ÷8.0m	14º30'	21.0m ÷ 23.0m	15º53'
	8.0m ÷11.0m	14º44'	23.0m ÷ 24.0m	15º39'
	11.0m ÷12.0m	15º25'	24.0m ÷26.0m	16º20'
	12.0m ÷14.0m	18º22'	26.0m ÷27.0m	17º41'

Table 3: The internal friction angle (ϕº) with Depths [12].

4.2 The Percentage of the Fine Particle and Water Content, Porosity, Saturation with Depths

4.2.1 Water Content with Depths

From Figure 2, it is easy to see that water content, saturation, and porosity varied remarkably with the different depths. The maximum value of the percentage of the fine clay particle obtained was 38% at 25.3m, which is according to water content (W%) of 25.6%; saturation (S) of 85.05%, and porosity of 44.49%. On the other hand, the minimum value of the percentage of the fine clay particle obtained 21% at 7.8m depth, which compared with the water content (W%) of 22.23%; saturation (S%) of 87.82%, and porosity (P%) of 40.55%.

Moreover, there is a special matter as the relationship between the percentage of the fine clay particle with W%; S%;, and P% evenly; which is 14.5%; 13.5%; 18%; 14%; 21%; 13%; 26.5%; 16%; 15.5%; 20%; 17%;12%; 35%; and 37% at 1.8m; 2.8m; 4.3m; 5.3m; 6.3m; 9.3m; 9.8m; 11.8m; 12.8m; 14.5m; 15.3m; 16.8m; 17.8m; 19.3m; 21.8m; and 22.8m; whereas compared with the W% of 23.22%; 22.25%; 23.962%; 22.89%; 21.89%; 22.23%; 21.4%; 23.1%; 21.38%; 22.46%; 22.93%; 21.12%; 21.8%; 21.46%; 20.82%; 22.79%; 23.9%; 24.32%; and P% of 42.63%; 40.62%; 4294%; 41.64%; 41.55%; 40.55%; 40.78%; 41.69%; 40.4%; 41.22%; 41.9%; 40.94%; 40.93%; 41.2%; 39.87%; 41.73%; 42.7%; and 43.72% (see Figure 2). So it is clear to conclude that the variation between the percentage of the fine clay particles and water content, saturation, and porosity are even. This resulted in the total volumetric strain (ε) not big value, so the soft clay ground is stable with the building loading.

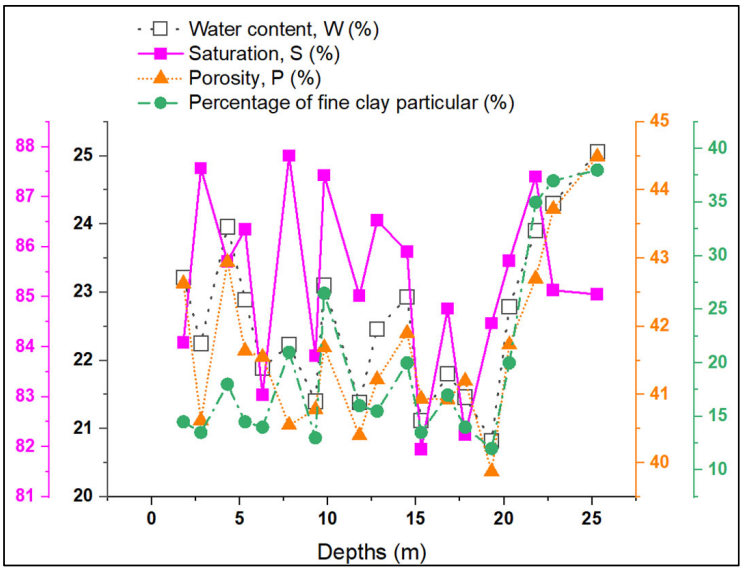

Figure 2: Results of the percentage of the fine clay particle and depths as consideration of the Water content, Saturation, Porosity

However, with (Thy Truc Doan, 2023), the research results by the experiment method presented water content with depths as consideration of the maximum value of the "HK2" at 4.8m, and decreases suddenly at 7.5m depth, and then become gradual stability as the in increasing of depths (see Figure 3).

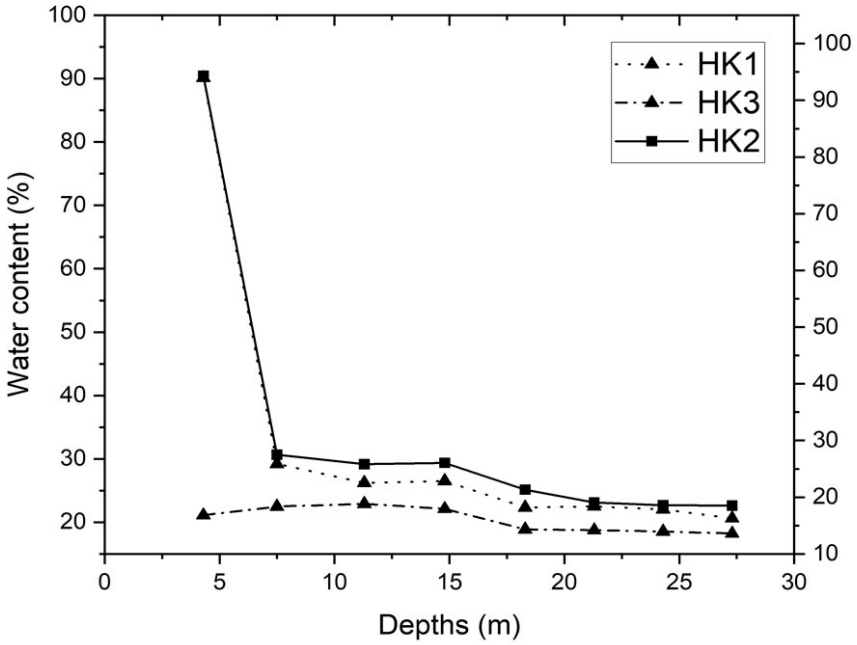

Figure 3: Water content (W%) was measured carefully at the different depths, which is shown from 0.0m to 27.0m at boreholes "HK1, HK2, HK3" (Thy Truc Doan, 2023)

4.2.2 Porosity with Depths

With (Thy Truc Doan, 2023), the research results by the experiment method presented porosity with depths such as:
Porosity is calculated by the formulas below:

$$P\%=(0.40+\eta)x\ 100\% \qquad (7)$$

Whereas, the value "0.40" shows soil with a standard porosity of 40% (η can be determined in Table 4).

The coefficient "η"	**Depths (m)**											
	Clay layer (The medium diameter is from <0.005mm to 0.5mm)								Sand layer (The medium diameter is from 0.2mm to 2.0mm)			
	0.0m ÷ 4.0m	4.0m ÷ 8.0m	8.0m ÷ 12.0m	12.0m ÷ 15.0m	15.0m ÷ 18.0m	18.0m ÷ 21.0m	21.0m ÷24.0m	24.0m ÷ 27.0m	27.0m ÷ 29.0m	29.0m ÷ 33.0m	33.0m ÷ 37.0m	37.0m ÷ 40.0m
	0.6	0.309	0.0567	0.0493	0.0406	0.0151	0.0163	0.0152	0.0064	0.0146	0.0168	0.0081
	0.6	0.319	0.0505	0.0471	0.004	0.0158	0.0242	0.0186	-	0.0125	0.0122	0.0085
	0.6	0.0684	-	-	-	-	-	-	-	0.0143	0.0109	-

Table 4: The coefficient "η" (Thy Truc Doan, 2023)

Results shew the Porosity (P%) has been obtained clearly at the maximum value of 71.9% (borehole "HK2") at 4.8m depth; whereas the minimum value is only 40.4%. At the ground level, porosity is bigger than in locations with increasing of 93.3m depth of 40.81%. The mean values at the center of the ground obtain 48.36 (see Figure 4).

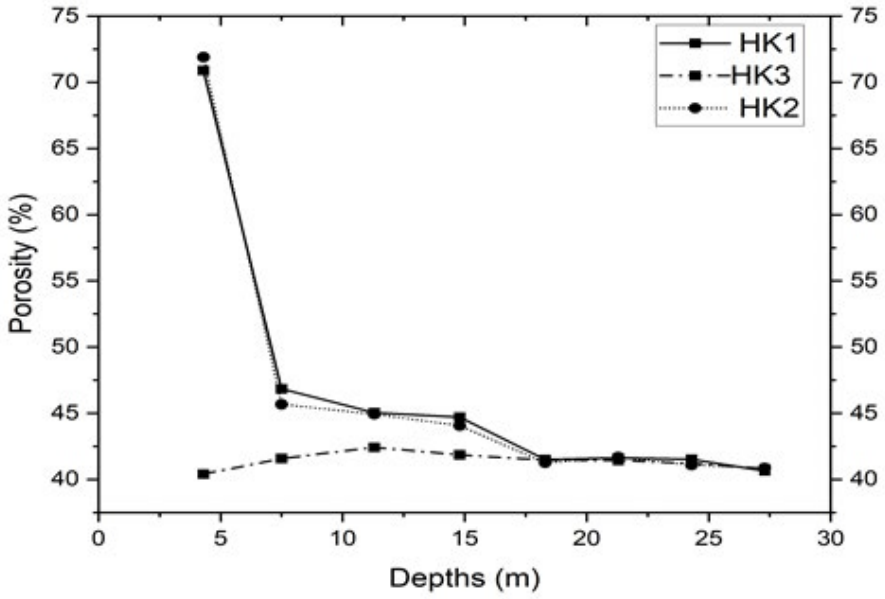

Figure 4: The Porosity (P%) has been shown clearly by the different Depths, which is from 0.0m to 27.0m at borehole "HK1, HK2, and HK3". Values varied relatively unevenly and decreased evenly as the increasing of depths." (Thy Truc Doan, 2023)

4.2.3 Saturation with Depths

With (Thy Truc Doan, 2023), the research results presented saturation with depths:
Saturation can be calculated by the formula below:

$$S\%=(0.7+\Delta)x\ 100\% \qquad (8)$$

Whereas the coefficient "0.7" show soil becomes a saturation state of 70% (see table 5).

The coefficient (Δ)	Depths (m)											
	Clay layer (The medium diameter is from <0.005mm to 0.5mm)								Sand layer (The medium diameter is from 0.2mm to 2.0mm)\			
	0.0m ÷ 4.0m	4.0m ÷ 8.0m	8.0m ÷ 12.0m	12.0m ÷ 15.0m	15.0m ÷ 18.0m	18.0m ÷ 21.0m	21.0m ÷24.0m	24.0m ÷ 27.0m	27.0m ÷ 29.0m	29.0m ÷ 33.0m	33.0m ÷ 37.0m	37.0m ÷ 40.0m
	0.3	0.2403	0.1918	0.1620	0.2036	0.1593	0.1499	0.1363	0.1095	0.1095	0.0131	0.0056
	0.3	0.2426	0.1707	0.1960	0.1492	0.1494	0.1366	0.1248	-	0.1144	0.1144	0.0169
	0.3	0.2036	-	-	-	-	-	-	-	0.0085	0.0154	-

Table 5: The coefficient "Δ" (Thy Truc Doan, 2023)

Results shew the increasing of saturation where is the location of the ground as the depth is low value; whereas compared with the increasing of depths with saturation decreased gradually (see Figure 5).

4.3 The Percentage of the Fine Clay Particle and Plasticity Index (IP), Viscosity (B) with Depths

Results of Figure 6, the percentage of the maximum value of fine clay particles is 38% at 25.3m depth of the viscosity (B) and plasticity index (Ip) with depths shown clearly and evenly as consideration of 25.06 and 85.05%. Whereas compared with the minimum value of 21% at 7.8m depth and according to the viscosity of 22.23 and plasticity of 87.82%. On the other hand, the percentage of fine clay particular 14.5%; 13.5%;18%; 14%; 13%; 26.5%;16%; 15.5%; 20%; 13.5%;17%; 12%; 35%; 37% at 1.8m; 2.8m; 4.3m; 5.3m; 6.3m; 9.3m; 9.8m; 11.8m; 12.8m; 14.5m; 15.3m; 16.8m; 17.8m; 19.3m; 21.8m; and 22.8m; which is according to 23.22; 22.25; 23.96; 22.89; 21.89; 22.23; 21.4; 23.1; 21.38; 22.46; 22.93; 21.12; 21.8; 21.46; 20.82; 23.9; 24.3; and plasticity index of 84.09%; 87.57%; 85.71%; 86.35%; 83.04%; 83.82%; 87.43%; 85.02%; 86.53%; 85.9%; 81.95%; 84.76%; 82.24%; 84.47%; 87.4%; and 85.13%. % (see Figure 6). So it is clear to conclude that the variation between the percentage of the fine clay particles and viscosity and plasticity index are even. This resulted in the total volumetric strain (ε) not big value, so the soft clay ground is stable with the building loading.

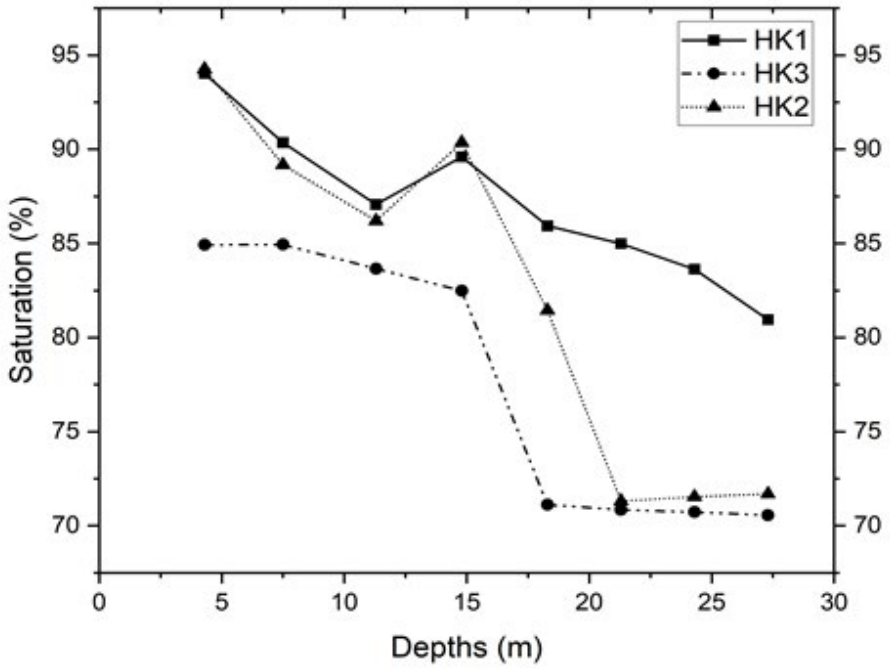

Figure 5: The Saturation (S%) of boreholes varied remarkably and unevenly as the increasing of the different Depths, which measured from 0.0m to 27.0m depths at boreholes HK1, HK2, and HK3". These differences have been shown clearly decreasing saturation as increasing of depth (Thy Truc Doan, 2023).

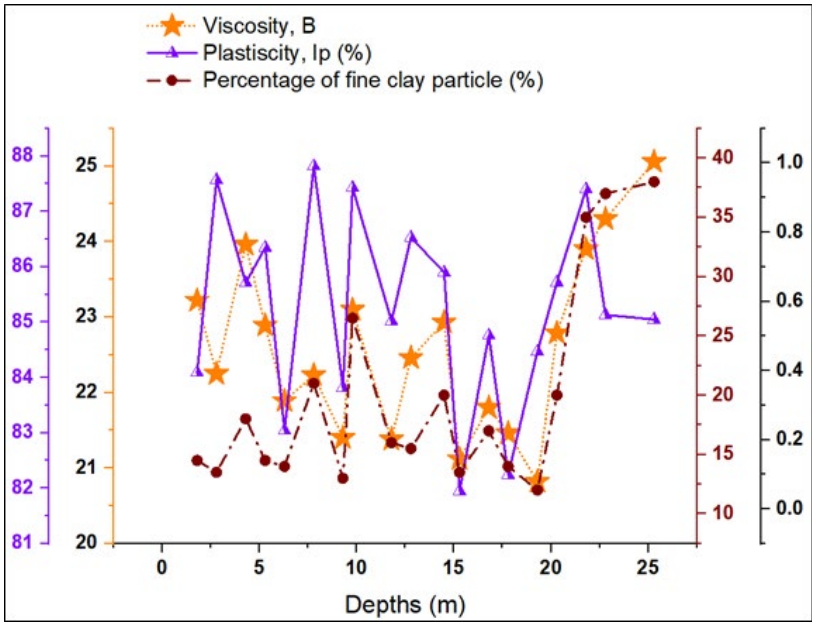

Figure 6: The percentage of the fine clay particle and Plasticity Index (IP), Viscosity (B) with depths

4.4 Simulation (Thy Truc Doan, 2023)

4.4.1 Data for Setting up the Model Simulation

a) Boundary conditions, assumptions, and limitations in the simulation

Simulation of the internal friction angle and depth variations by the PLAXIS 3D software (the finite element method) was designed by the Mohr-Coulomb theory model. The parameters E', ν', φ', ψ' are assumpted in Table 6 and Figure 7. The ground is soft clay from 0.0m to 25.3m. The groundwater level is at +0.3m.

b) Mesh and loading

Mesh is divided into the full surface of the model to simulate fully around on the ground (see Table 6). The building loading is considered as completely stiff with reinforcement concrete materials and putting on the full surface and it is the same as evenly loading. At the initial state, the model worked with no loading, whereas at the second state active loading created a dangerous state on the ground.

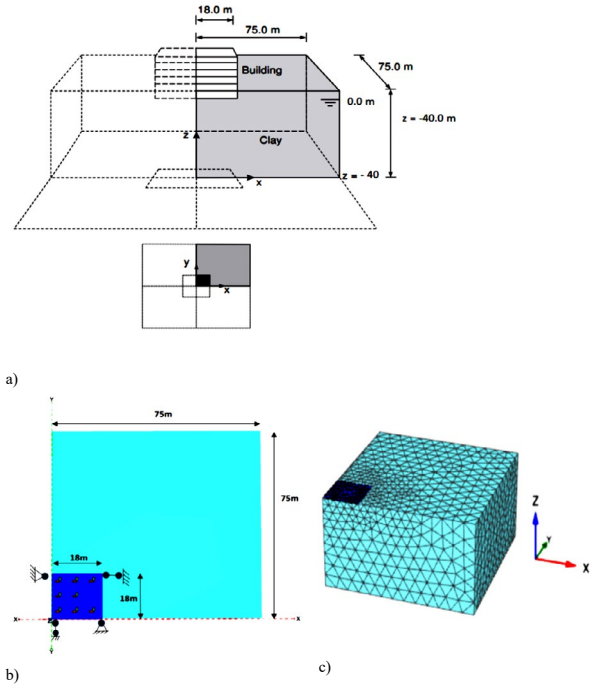

Figure 7: (a, b) The boundary condition and active loading; (c) mesh division of the model simulation (Thy Truc Doan, 2023)

Descriptions	Signs	Value	Unit
Soil properties			
Unit weight above the groundwater level	γusat	18.2 (Clay layer)	kN/m3
Unit weight above the groundwater level	γsat	18.9 (Clay layer)	kN/m3
Young's modulus (constant)	E'	1.104	kN/m2
Poisson's ratio	ν'	0.3	-
Cohesion (constant)	C'ref	30.2	kN/m2
Internal friction angle	Ɵ	18.48	(0)
Lateral earth pressure coefficient	K0	0.5	-
Stiffness	E''	1.103	kN/m2
Structure material properties			
Stiffness	ν'(nu)	0.3	-
Strength	c'ref	30.2	kN/m2
Thickness	d	-	m
Weight	γ	50	kN/m3
Young's modulus	E1	3.107	kN/m2
Poisson's ratio	ν12	0.15	-

Table 6: Parameter and properties of materials to set up the software with the medium values [13].

c) Results of output data of the simulation

Results in Figure 7 show the percentage of the fine clay particle and the total volumetric strain (ε) with depths. The minimum value of 12% and 0.00002617 at 19.3m depth; whereas the maximum value of 38% and 0.00002609 at 25.3m depth. Moreover, the total volumetric strain varied evenly with the percentage of the fine clay particles; which shows 14.5%; 13.5%; 18%; 14%; 21%; 13%; 26.5%; 16%; 15.5%; 20%; 13.5%; 17%; 12%; 35%; and 37%; compared with 0.00002606; 0.00002612; 0.00002603; 0.00002612; 0.00002609; 0.00002613; 0.0000261; 0.00002612; 0.00002612; 0.0000261; 0.00002617; 0.00002612; 0.00002606; and 0.0000261 (see Figure 8).

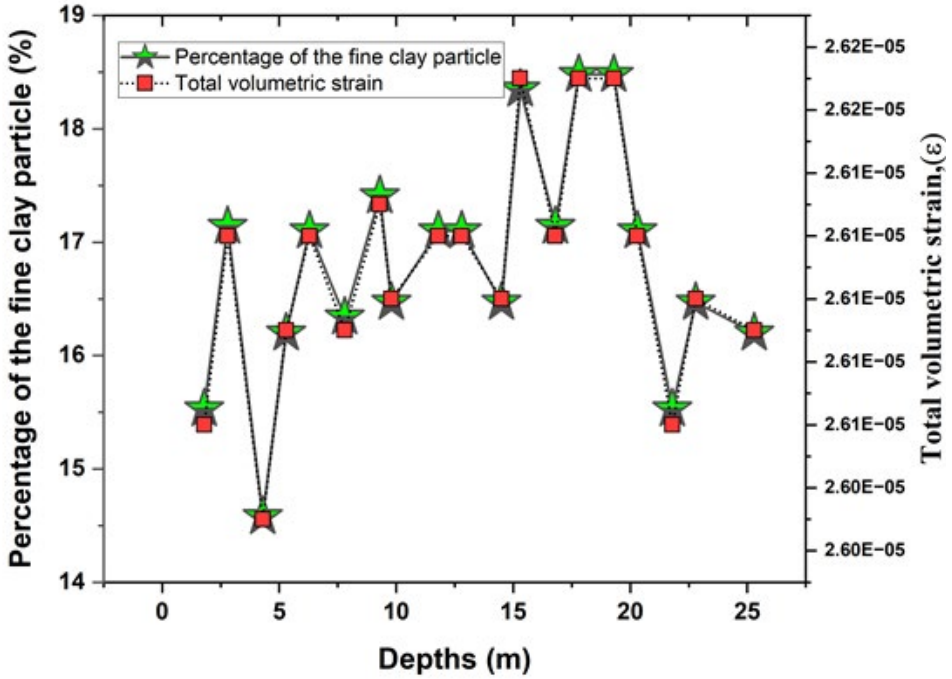

Figure 8: Results of simulation of the percentage of the fine clay particle and Total volumetric strain (ε) with depths

5. Conclusions

Influence evaluation of the percentage of fine particles of marine clay at the different depth variations to the total volumetric strain of the soft clay ground is determined by the Viet Nam standard TCVN 4196:2012; TCVN 4102:2012; TCVN 4197:2012; TCVN 4199:2012. Results show clearly as a consideration of the relationship between Internal friction angle, Cohesive force, Water content, Saturation, Porosity, Viscosity, and Plasticity index with depths. The variations of the percentage of fine particles of marine clay at the different depth variations to the total volumetric strain of the soft clay ground are stable and safe state to use and design the building and construction.

Moreover, the soft clay soil with the marine original is also deformed stability although the groundwater level variations are clear. However, the soft ground needs to consider the other evaluation of the percentage of fine clay particles, because with fine clay particles usually occur more so it is easier to deform deformation under heavy loading with the groundwater level is at the ground.

Conflict of Interest

I certainly do not have any conflicts of interest with anyone in the results of this article.

This result is my own product during the time of research and discovery. If there is anything wrong with this guarantee, I take full responsibility for the policy of the Journal.

References

1. Arroyo, H., Rojas, E., de la Luz Perez-Rea, M., Horta, J., & Arroyo, J. (2015). A porous model to simulate the evolution of the soil–water characteristic curve with volumetric strains. Comptes Rendus Mécanique, 343(4), 264-274.
2. Arumugam, H., Ahn, C. H., Rimdusit, S., & Muthukaruppan, A. (2023). Development of high performance granite fine fly dust particle reinforced epoxy composites: structure, thermal, mechanical, surface and high voltage breakdown strength properties. Journal of Materials Research and Technology, 24, 2795-2811.
3. Elrahmani, A., Al-Raoush, R. I., Abugazia, H., & Seers, T. (2022). Pore-scale simulation of fine particles migration in porous media using coupled CFD-DEM. Powder Technology, 398, 117130.
4. Ekop, I. E., Okeke, C. J., & Inyang, E. V. (2022). Comparative study on recycled iron filings and glass particles as a potential fine aggregate in concrete. Resources, Conservation & Recycling Advances, 15, 200093.
5. Gaetano, D., Greco, F., Leonetti, L., Blasi, P. N., & Pascuzzo, A. (2022). A hybrid cohesive/volumetric multiscale finite element model for the failure analysis of fiber-reinforced composite structures. Procedia Structural Integrity, 41, 439-451.
6. Lin, J., Zou, W., Han, Z., Zhang, Z., & Wang, X. (2022). Structural, volumetric and water retention behaviors of a compacted clay upon saline intrusion and freeze-thaw cycles. Journal of Rock Mechanics and Geotechnical Engineering, 14(3), 953-966.
7. Party, P., Kókai, D., Burián, K., Nagy, A., Hopp, B., & Ambrus, R. (2022). Development of extra-fine particles containing nanosized meloxicam for deep pulmonary delivery: In vitro aerodynamic and cell line measurements. European Journal of Pharmaceutical Sciences, 176, 106247.
8. Tudisco, E., Hall, S. A., Charalampidou, E. M., Kardjilov, N., Hilger, A., & Sone, H. (2015). Full-field measurements of strain localisation in sandstone by neutron tomography and 3D-volumetric digital image correlation. Physics Procedia, 69, 509-515.
9. Wei, Y. (2012). An extended strain energy density failure criterion by differentiating volumetric and distortional deformation. International Journal of Solids and Structures, 49(9), 1117-1126.
10. Kardani, N., Zhou, A., Nazem, M., & Shen, S. L. (2021). Improved prediction of slope stability using a hybrid stacking ensemble method based on finite element analysis and field data. Journal of Rock Mechanics and Geotechnical Engineering, 13(1), 188-201.
11. Wang, T., Zhai, Y., Gao, H., Li, Y., & Zhao, R. (2023). A novel binary effective medium model to describe the prepeak stress–strain relationship of combined bodies of rock-like material and rock. International Journal of Mining Science and Technology.
12. Truc Doan, T. (2023). Finite element method of the internal friction angle and saturation degree with the groundwater levels variations. Geology, Ecology, and Landscapes, 1-22.
13. Brinkgreve, R. B. J., Kumarswamy, S., Swolfs, W. M., Waterman, D., Chesaru, A., & Bonnier, P. G. (2016). PLAXIS 2016. PLAXIS bv, the Netherlands.